



CHORUS

This is the accepted manuscript made available via CHORUS. The article has been published as:

First-principles multiple-barrier diffusion theory: The case study of interstitial diffusion in CdTe

Ji-Hui Yang, Ji-Sang Park, Joongoo Kang, and Su-Huai Wei

Phys. Rev. B **91**, 075202 — Published 17 February 2015

DOI: [10.1103/PhysRevB.91.075202](https://doi.org/10.1103/PhysRevB.91.075202)

First-principles Multi-barrier Diffusion Coefficient Theory: the Case Study of Interstitial Diffusion in CdTe

Ji-Hui Yang¹, Ji-Sang Park¹, Joongoo Kang^{2*}, and Su-Huai Wei^{1*}

¹National Renewable Energy Laboratory, Golden, CO 80401, USA

²Department of Emerging Materials Science, DGIST, Daegu 711-873, Korea

Abstract

Diffusion of particles in solid-state materials generally involves several sequential thermal-activation processes. However, present diffusion coefficient theory only deals with single barrier, i.e., it lacks an accurate description to deal with such multi-barrier diffusion. Here, we develop a general diffusion coefficient theory for multi-barrier diffusion. Using our diffusion theory and first-principles calculated hopping rates for each barrier, we calculate the diffusion coefficients of Cd, Cu, Te, and Cl interstitials in CdTe for their full multi-barrier diffusion pathways. We found that the calculated diffusivity agrees well with the experimental measurement, thus justifying our theory, which is general for many other systems.

PACS number(s): **66.30.Dn, 66.30.H-, 61.72.jj, 61.72.uj**

I. INTRODUCTION

Diffusion of ions in functional materials is crucial in many applications such as lithium-ion batteries [1-3] and transition-metal-based resistive random access memory materials [4, 5]. In photovoltaic and microelectronic materials, dopants (especially external impurities) are often introduced by a diffusion process [6, 7]. Thus, the control of ion diffusion is important for the performance of semiconductor devices. Although various mechanisms of ion diffusions exist at the atomic scale, such as interstitialcy, kick-out and the vacancy mechanisms [8-11], macroscopically, the ion diffusion process can be well described by Fick's laws [12]. In a homogenous media, the particle diffusion equation in 1-dimension is written as $\frac{\partial \rho}{\partial t} = D \frac{\partial^2 \rho}{\partial x^2}$, where ρ is particle density and D is diffusion coefficient, which is usually described by an Arrhenius relation [13], i.e., $D = D_0 \exp(-E_a/k_B T)$, where D_0 is the pre-factor, and E_a is the energy barrier between a local minimum and a saddle point (transition state) in the diffusion pathway. T and k_B in the equation are temperature and the Boltzmann constant, respectively. Experimentally, D_0 is usually extracted from ion diffusion profiles by fitting Arrhenius relation. However, due to coexistence of possible different diffusion mechanisms, this kind of extraction can vary significantly and understanding of experimental data will require comparison with theoretical calculations. Theoretically, first-principles calculations are commonly used to get the diffusion paths and barriers. But the diffusion coefficients are difficult to calculate. Previous works has either adopted (semi)empirical approaches [14–17], which is not very accurate, or adopted classical ab initio molecular dynamics simulation techniques [18–20], which usually is very computationally intensive. Recently, transition state theory has been combined with first-principles methods to calculate diffusion coefficients with great success [21], but it is only for diffusion process with single energy barrier. However, ion diffusion in solid-state media generally involves multi-barriers associated with sequential hopping processes. For example, the diffusion pathways of Cu and Cd interstitials in CdTe have two energy barriers [22]. As a matter of fact, multi-barrier diffusion is prevalent in a variety of functional

materials. To our knowledge, however, there is no diffusion coefficient theory and theoretical calculations of diffusion coefficients are lacking for systems with multi-barriers, which highlight the requirement to develop a method to address multi-barrier diffusion coefficient problem.

In this paper, we first develop a diffusion coefficient theory for multi-barrier diffusion processes using Monte Carlo (MC) simulations. Then, as an example of multi-barrier diffusion, we calculate the diffusion coefficients of Cu_i , Cd_i , Te_i , and Cl_i interstitials in CdTe based on our theory. As is well known that Cu and Cl treatments are necessary to produce high-efficiency polycrystalline CdTe solar cells [23-25], and generally, Cu and Cl are introduced into CdTe through diffusion. The diffusion of Cd and Te in CdTe is also of great interest because they exist naturally in the host and may be involved in the Cu and Cl diffusion process. The diffusion of these elements often involves complicated pathways with more than one barrier. Therefore, the diffusion coefficients can only be dealt with using multi-barrier diffusion coefficient theory.

II. MULTI-BARRIER DIFFUSION COEFFICIENT THEORY

Before studying multi-barrier cases, we first briefly discuss diffusion in a one-dimensional lattice where all the sites are equivalent and a particle can hop to one of its nearest-neighbor sites with rate h , as shown in Fig. 1. In this case, the particle density ρ_i at the site i changes with time following the equation:

$$\frac{\partial \rho_i}{\partial t} = h(\rho_{i+1} + \rho_{i-1}) - 2h\rho_i = a^2 h \frac{\partial^2 \rho_i}{\partial x^2} . \quad (1)$$

Here, a is diffusion length, which is the distance between the neighboring sites. In the continuum limit and compared to Fick's second law, the diffusion coefficient D is then given by $D = a^2 h$, in agreement with the formula derived from transition state theory [26, 27]. Here, according to dynamical matrix theory [27], the hopping rate h is given by $h = \mu \exp(-E_a/k_B T)$, where μ is the attempting frequency of particle hopping. In harmonic approximation, μ can be calculated as:

$$\mu = \frac{\sum_{i=1}^{3N-3} \omega_i}{\sum_{j=1}^{3N-4} \omega_j} \quad (2)$$

where ω_i are $3N - 3$ positive phonon frequencies at the local minimum configuration and ω_j are $3N - 4$ positive phonon frequencies at the saddle-point.

We now turn to the case with multi-barriers. Here, we first present our results for diffusion with two barriers, and it can be easily generalized to the cases with more barriers, as we will show later. Figure 2 shows one-dimensional lattice models for two-barrier diffusion. The unit cell of the lattice contains two sublattice sites, black and grey, and each of them is indexed by i and j , respectively. Without losing generality, we assign h_2 and h_1 for the hopping events from the site i to j and from the site j to $i + 1$, respectively. There are two different types of diffusion on the two-barrier diffusion model: for type-I diffusion [Fig. 2(a)], the subsequent particle hopping occurs from the site $i + 1$ to j at rate h_1 and from the site j to i at rate h_2 . On the other hand, for type-II diffusion [Fig. 2(b)], the same subsequent hopping events involve h_2 first and h_1 later. Notice that here we assume the particle is diffusing in a uniform media, so the whole diffusion path is symmetric, i.e., there is no drift motion of particles in the system. As we will see later, Cu_i diffusion in CdTe is type-I, whereas Cd_i diffusion is type-II. For type-I diffusion, the diffusion of particles is described by the pair of hopping equations:

$$\begin{aligned} \frac{\partial \rho_i}{\partial t} &= h_1 \rho_{j-1} + h_2 \rho_j - (h_1 + h_2) \rho_i, \\ \frac{\partial \rho_j}{\partial t} &= h_2 \rho_i + h_1 \rho_{i+1} - (h_1 + h_2) \rho_j. \end{aligned} \quad (3a)$$

Similarly, the governing equations for type-II diffusion are given as:

$$\begin{aligned} \frac{\partial \rho_i}{\partial t} &= h_1 \rho_{j-1} + h_1 \rho_j - 2h_2 \rho_i, \\ \frac{\partial \rho_j}{\partial t} &= h_2 \rho_i + h_2 \rho_{i+1} - 2h_1 \rho_j. \end{aligned} \quad (3b)$$

Regardless of microscopic details of particle motions, diffusion of particles in a uniform medium is generally described by the diffusion equation, $\frac{\partial \rho}{\partial t} = D \nabla^2 \rho$, at the continuum level. Our lattice model also is uniform and symmetric. We performed Monte Carlo simulations to describe the probability distributions $\rho_i(t)$ and $\rho_j(t)$ of a

particle at the sublattice sites i and j , respectively, starting from a particle at $i = 0$ and $t = 0$. Because we are interested in the particle distribution at a large length scale, we only take the black sublattice as a coarse-grained lattice model and define the average particle density ρ_i^{ave} on the site i as $\rho_i^{ave} = \rho_i + (\rho_{j-1} + \rho_j)/2$. After transient Monte-Carlo steps, the Gaussian distribution of $\rho_i^{ave}(t)$ emerges with $\langle x^2 \rangle = 2Dt$. Our MC simulations reveal that from the microscopic particle motions governed by Eq. (3), the diffusion equation emerges after transient particle redistribution. As the MC simulation time increases, the time evolution of the ρ_i^{ave} in the coarse-grained lattice model can be described by the simple diffusion equation. We found that there exists a function f that bridges the macroscopic diffusion coefficient D and the microscopic hopping rates as follows:

$$D = \left(\frac{a}{2}\right)^2 \sqrt{h_1 h_2 f\left(\frac{h_2}{h_1}\right)}. \quad (4)$$

Here, f renormalizes the effective hopping rate for the coarse-grained diffusion model. We note that f depends only on the ratio of h_2/h_1 , but not on the absolute values of h_1 and h_2 (Fig. 3). For the two-barrier case, the renormalization factor f turns out to be identical for both type-I and type-II diffusion models in Fig. 2. However, we found that for n -barrier cases with $n > 2$, f is generally different for different diffusion types.

We can rationalize the form of f in Fig. 3 in the two limiting cases. (i) For $h_1 = h_2 = h$, the two-barrier diffusion model is reduced to the one-barrier diffusion in Fig. 1 with the diffusion length of $a/2$. Thus, $D = (a/2)^2 h$, in consistent with $f(1) = 1$ in Eq. (4). (ii) For $h_2 \ll h_1$, f is approximated to $4h_2/h_1$, and D can be analytically written as $a^2 h_2/2$. The factor $1/2$ in D can be understood as follows: for the type-I case, a particle moves rapidly back and forth between site i and site $j - 1$ (or equivalent site pairs) with large hopping rate of h_1 [Fig. 4(a)]. If we regard site i and site $j - 1$ as one site as denoted by 2 in Fig. 4(a), the diffusion equation can be written as $\partial(\rho_i + \rho_{j-1})/\partial t = h_2 \rho_{i-1} + h_2 \rho_j - h_2 (\rho_i + \rho_{j-1})$. Because the barrier between site i and $j - 1$ is very small, the particles are expected to move very fast

between these two sites, therefore, we should have $\rho_i = \rho_{j-1}$ and $\rho_j = \rho_{i+1}$. Finally we have $2\partial\rho_i/\partial t = h_2 \rho_{i-1} + h_2 \rho_{i+1} - 2h_2\rho_i = a^2 h_2 \partial^2 \rho_i / \partial x^2$ or $\partial\rho_i/\partial t = \frac{1}{2} a^2 h_2 \partial^2 \rho_i / \partial x^2$. Therefore, the share of particles between site i and $j - 1$ reduces half of hopping particle densities and gives the diffusion coefficient analytically as $D = a^2 h_2 / 2$. Generally, the share of particles among N connected sites between large barriers reduces the effective hopping rate by $1/N$. For the type-II case, the effective rate for the hopping from site i to site $i + 1$ will be reduced by half, because a particle at site j will move forward or backward with equal chance [Fig. 4(b)]. In this case, the diffusion equation is $\partial\rho_i/\partial t = \frac{h_2}{2} \rho_{i-1} + \frac{h_2}{2} \rho_{i+1} - 2\frac{h_2}{2} \rho_i = a^2 \frac{h_2}{2} \partial^2 \rho_i / \partial x^2$ or $\partial\rho_i/\partial t = \frac{1}{2} a^2 h_2 \partial^2 \rho_i / \partial x^2$. As a result, the diffusion coefficient is reduced by half and has the analytical form $D = a^2 h_2 / 2$. However, except the limited cases discussed above, the function $f(h_2/h_1)$ in Eq. (4) needs to be calculated using MC simulation. The numerical data is plotted in Fig. 3. Thus, Eq. (4) provides a general formula and numerical solution for two-barrier diffusion coefficient problems and will greatly simplify future calculation of diffusion coefficient of multi-barrier system.

For three-barrier diffusion, our MC simulations show that the diffusion coefficient D is given by:

$$D = \left(\frac{a}{3}\right)^2 \left[h_1 h_2 h_3 f\left(\frac{h_2}{h_1}, \frac{h_3}{h_1}\right) \right]^{1/3}, \quad (5)$$

which is a generalization of Eq. (4). Here, the renormalization factor f now depends on the two ratios of the hopping rates. The generalization for n -barrier cases with $n > 3$ would be straightforward. In many practical cases, however, there exist only one or two dominant energy barriers among the n barriers in a full diffusion pathway. When h_3 is much smaller than other $n - 1$ hopping rates, i.e., the barrier associated with h_3 is much larger than the others, the n -barrier diffusion can be reduced to one-barrier diffusion, as we demonstrated for $n = 2$ in Fig. 4: the share of particles among N connected sites between large barriers reduces the diffusion coefficient by $1/N$ [Fig. 4(a)], whereas a diffusion plateau reduces it by half regardless of the number of sites at the plateau [Fig. 4(b)]. Likewise, when two hopping rates are much smaller than

others, the n-barrier diffusion can be reduced to two-barrier diffusion.

Note that for three-dimensional diffusion, the diffusion coefficient discussed above should be multiplied by $z/6$, where z is the number of diffusion paths accessible from a given site [28,29]. The diffusion length should be the total distance that a particle moves in a full diffusion path.

III. FIRST-PRINCIPLES CALCULATION METHOD

To get the hopping rate for a single barrier, first-principles calculations are performed using density functional theory (DFT) [30,31] as implemented in the VASP code [32,33]. The electron and core interactions are included using the frozen-core projected augmented wave (PAW) approach [34]. The initial atomic configurations of local minimum sites and saddle points were adopted from previous works [22], which were calculated using the generalized gradient approximation (GGA) formulated by Perdew, Burke, and Ernzerhof (PBE) [35]. To correct the bandgap error in the GGA calculation, we used the Heyd-Scuseria-Ernzerhof (HSE06) hybrid functionals [36] ($\alpha=0.25$) and nudged elastic band (NEB) method [37] to get the diffusion barriers for the full diffusion paths. We find that local minimum and saddle-point configurations are almost the same before and after the bandgap corrections. As a result, the zone-centered phonon frequencies at the minimum sites and saddle points are calculated within the PBE framework by making finite displacements (0.015 Å) in these structures. An energy cut-off of 350 eV and a Gamma-centered k-point mesh $2\times 2\times 2$ are used. To reduce computational costs, for each barrier, only atoms within 5 Å from the diffuser are allowed to move and other atoms are frozen. Our test results for Te_i diffusions show that the attempting frequencies obtained this way are similar with those obtained by allowing all phonons.

IV. RESULTS AND DISCUSSIONS

Figure 5 shows the diffusion paths of Cu, Cd, Te, and Cl interstitials in CdTe. Compared to PBE diffusion paths in Ref. 22, we found that HSE06 strengthened spin splitting, making Bc configuration of neutral Cl interstitial about 0.26 eV smaller than

Tc site. All the other diffusions are similar to PBE results except for neutral Cu interstitial. In Cu_i case, HSE06 corrected the band gap of CdTe, thus reducing the s-d coupling, and consequently reduce the energy difference between Tc' site and m site as explained in Ref. 38.

Table 1 lists our calculated results of diffusion parameters for Cu_i, Cd_i, Te_i, Cl_i and their charged states. The attempting frequencies are only listed for the hopping with the highest barriers in their diffusion paths. Our results show that, for diffusions of Cu_i, Cu_i⁺, Cd_i, Cd_i²⁺, and Cl_i⁻, although they all have two barriers, the hopping rates h_2 of the larger barriers are actually much smaller than those h_1 of the smaller barriers. Take Cu_i as an example: the attempting frequency of the small barrier (0.05 eV) is 2.84 THz and the attempt frequency of the high barrier (0.28 eV) is 4.19 THz. According to our definition of hopping rate above, we have $h_1 = 2.84 \exp(-0.05 \text{ eV}/k_B T)$ THz and $h_2 = 4.19 \exp(-0.28 \text{ eV}/k_B T)$ THz. At the usual growth temperature, T is less than 1000 K, so h_2/h_1 is less than 0.15 and the linear approximation of function $f(h_2/h_1)$ is enough to describe the full-path diffusion coefficient D , which is $\frac{z}{6} a^2 h_2 / 2 = \frac{z}{12} a^2 \mu \exp(-E_a/k_B T) = D_0 \exp(-E_a/k_B T)$. Here, D_0 , which equals $z/12 a^2 \mu$ is the effective diffusion coefficient pre-factor for a two-barrier diffusion. Notice that, compared to one-barrier diffusion, D_0 is reduced by half. For diffusions of Te_i and Te_i²⁺, since they are both one-barrier diffusions, their diffusion coefficients D are simply $D_0 \exp(-E_a/k_B T)$ with $D_0 = z/6 a^2 \mu$. For Cl_i⁻ diffusion, which involves three barriers, the effective diffusion coefficient pre-factor will be $D_0 = z/24 a^2 \mu$.

Using our calculated effective energy barriers and effective diffusion coefficient pre-factors, we can get the diffusion coefficients of these defects at a given temperature. For example, at T=800 K, Cd_i has a diffusion coefficient of $9.07 \times 10^{-7} \text{ cm}^2/\text{s}$ and Cd_i²⁺ has a diffusion coefficient of $3.65 \times 10^{-6} \text{ cm}^2/\text{s}$. Our theoretical result agrees very well with the experimental measurement for Cd_i, which is $1.75 \times 10^{-6} \text{ cm}^2/\text{s}$ [39]. For Cu_i and Cu_i⁺, the calculated diffusion coefficients at T=800 K are $6.22 \times 10^{-5} \text{ cm}^2/\text{s}$ and $8.28 \times 10^{-6} \text{ cm}^2/\text{s}$, respectively. The

calculated results indicate that Cu diffuses faster than Cd, which can be explained by the strong s-d coupling for Cu [38]. The experimental reported value [40] of Cu diffusion in CdTe is quite small with $D = 6.65 \times 10^{-5} \text{ cm}^2\text{s}^{-1} \exp(-0.57 \text{ eV}/k_B T)$ or $2.6 \times 10^{-8} \text{ cm}^2/\text{s}$ at $T=800 \text{ K}$. This small experimental value might be because the measured result is not just for Cu interstitials but also involves other Cu diffusion mechanisms, such as through Cd vacancy, Cu_{Cd} . When Cu is trapped at Cd site, it has a much smaller diffusion coefficient. This speculation is consistent with recent experimental observations [41]. We notice that the diffusion coefficient of Ag_i , which is experimentally measured to be $8.4 \times 10^{-6} \text{ cm}^2/\text{s}$ under Te-rich and $2.0 \times 10^{-5} \text{ cm}^2/\text{s}$ under Cd-rich conditions [39], has diffusion coefficients similar to our calculated value. We suggest that more studies on the Cu interstitial diffusions are needed.

Our results shown in Table 1 indicate that the diffusion properties are actually very sensitive to the charge states of these interstitial atoms. Neutral Cu_i diffuses much faster than Cu_i^+ , and Cl_i diffuses faster than Cl_i^- . Generally, the charge states of these defects are determined by the Fermi level in CdTe. For the case of Cu_i , it has a (0/+) transition energy level of 0.14 eV below the conduction-band minimum (CBM) of CdTe (Fig. 6). Under Cd-rich conditions, the system will be more n-type, i.e., the Fermi level will be closer to the CBM; thus, there will be more neutral Cu_i and the diffusion of Cu is expected to be enhanced. In contrast, under Te-rich conditions, the Fermi level will be closer to the valence-band minimum (VBM) of CdTe; thus, more Cu_i will become ionic and the diffusion will be slowed. The same arguments can explain why experimental results show that Ag_i diffuses faster under Cd pressure than under Te pressure. For Cl_i , because it has (0/-) transition level at 0.17 eV above the VBM of CdTe, we can expect that it will diffuse faster under Te pressure than under Cd pressure, with its diffusion coefficient varying between $8.50 \times 10^{-6} \text{ cm}^2/\text{s}$ and $3.14 \times 10^{-8} \text{ cm}^2/\text{s}$ at 800 K. For Te_i , although it has a much faster diffusion of $1.51 \times 10^{-4} \text{ cm}^2/\text{s}$ at 800 K, experimentally, there is no clear evidence showing that Te diffuses faster than Cd. This could be due to two reasons. First, at Te-rich conditions with the Fermi level close to VBM, most of the Te_i become ionized with a

smaller diffusion coefficient of $7.54 \times 10^{-6} \text{ cm}^2/\text{s}$. Second, at Cd-rich conditions, the formation energy of Te_i will be very high; thus, there could be a very small amount of Te_i for observation. More accurate experimental measurements may be required to confirm this.

IV. CONCLUSIONS

In conclusion, we have developed a theory to easily calculate the diffusion coefficients for multi-barrier diffusion process. Using this theory, we studied the diffusion properties of Cu_i , Cd_i , Te_i , Cl_i in CdTe and their charge-state dependences. Our theoretical results provided a deep understanding on the diffusion mechanism of these defects in CdTe which are important for improvement of the stability and performance of CdTe solar cells. Our theory on the diffusion coefficient is general and can be applied to study many other diffusion processes with multi-barriers.

ACKNOWLEDGMENTS

The work at NREL was funded by the U.S. Department of Energy under Contract No. DE-AC36-08GO28308. The work at DGIST was supported by the DGIST MIREBrain Program. The calculations were done on NREL's Peregrine supercomputer and at the National Energy Research Scientific Computing Center, which is supported by the Office of Science of the U.S. Department of Energy under Contract No. DE-AC02-05CH11231.

e-mail: joongoo.kang@dgist.ac.kr

e-mail: Suhuai.Wei@nrel.gov

- [1] J.-M. Tarascon and M. Armand, *Nature* **414**, 359 (2001).
- [2] V. Meunier, J. Kephart, C. Roland, and J. Bernholc, *Phys. Rev. Lett.* **88**, 075506 (2002).
- [3] J. Sugiyama, K. Mukai, Y. Ikedo, H. Nozaki, M. Månsson, and I. Watanabe, *Phys. Rev. Lett.* **103**, 147601 (2009).
- [4] R. Waser and M. Aono, *Nature Materials* **6**, 833 (2007).
- [5] Y. B. Nian, J. Strozier, N. J. Wu, X. Chen, and A. Ignatiev, *Phys. Rev. Lett.* **98**, 146403 (2007).
- [6] International Technology Roadmap for Semiconductors (Semiconductor Industry Association, 2005), <http://www.itrs.net/Common/2005ITRS/Home2005.htm>.
- [7] D. D. Salvador, E. Napolitani, S. Mirabella, G. Bisognin, G. Impellizzeri, A. Carnera, and F. Priolo, *Phys. Rev. Lett.* **97**, 255902 (2006).
- [8] B. Sadigh, T. J. Lenosky, S. K. Theiss, M.-J. Caturla, T. D. de la Rubia, and M. A. Foad, *Phys. Rev. Lett.* **83**, 4341 (1999).
- [9] I. Suarez-Martinez, A. A. El-Barbary, G. Savini, and M. I. Heggie, *Phys. Rev. Lett.* **98**, 15501 (2007).
- [10] N. E. B. Cowern, G. F. A. van de Walle, D. J. Gravesteijn, and C. J. Vriezema, *Phys. Rev. Lett.* **67**, 212 (1991).
- [11] G.-D. Lee, C. Z. Wang, E. Yoon, N.-M. Hwang, D.-Y. Kim, and K. M. Ho, *Phys. Rev. Lett.* **95**, 205501 (2005).
- [12] http://en.wikipedia.org/wiki/Fick's_laws_of_diffusion
- [13] P. E. Blöchl, E. Smargiassi, R. Car, D. B. Laks, W. Andreoni, and S. T. Pantelides, *Phys. Rev. Lett.* **70**, 2435 (1993).
- [14] P. A. Varotsos and K. D. Alexopoulos, *Thermodynamics of Point Defects and Their Relation with Bulk Properties* (North-Holland, Amsterdam, 1986).
- [15] G. Neumann, *Phys. Status Solidi B* **144**, 329 (1987).
- [16] J. B. Adams, *J. Mater. Res.* **4**, 102 (1989).
- [17] W. Frank et al., *Phys. Rev. Lett.* **77**, 518 (1996).

- [18] P. E. Blochl et al., Phys. Rev. Lett. **70**, 2435 (1993).
- [19] N. Sandberg, B. Magyari-Kope, and T. R. Mattsson, Phys. Rev. Lett. **89**, 065901 (2002).
- [20] V. Milman et al., Phys. Rev. Lett. **70**, 2928 (1993).
- [21] M. Mantina, Y. Wang, R. Arroyave, L. Q. Chen, and Z. K. Liu, Phys. Rev. Lett. **100**, 215901 (2008).
- [22] J. Ma, J. Yang, S.-H. Wei, and J. L. F. Da Silva, Phys. Rev. B **90**, 155208 (2014).
- [23] D. H. Rose, F. S. Hasoon, R. G. Dhere, D. S. Albin, R. M. Ribelin, X. S. Li, Y. Mahathongdy, T. A. Gessert, and P. Sheldon, Prog. Photovolt: Res. Appl. **7**, 331 (1999).
- [24] L. Zhang, J. L. F. Da Silva, J. Li, Y. Yan, T. A. Gessert, and S.-H. Wei, Phys. Rev. Lett. **101**, 155501 (2008).
- [25] J. Ma, S.-H. Wei, T. A. Gessert, and K. K. Chin, Phys. Rev. B **83**, 245207 (2011).
- [26] H. Eyring, J. Chem. Phys. **3**, 107 (1935).
- [27] G. H. Vineyard, J. Phys. Chem. Solids **3**, 121 (1957).
- [28] F. Agullo-Lopez, C. Catlow, and P. Townsend, Point Defects in Materials (Academic Press, London, 1988).
- [29] F. El-Mellouhi, N. Mousseau, and P. Ordejón, Phys. Rev. B **70**, 205202 (2004).
- [30] P. Hohenberg and W. Kohn, Phys. Rev. **136**, B864 (1964).
- [31] W. Kohn and L. J. Sham, Phys. Rev. **140**, A1133 (1965).
- [32] G. Kresse and J. Furthmüller, Phys. Rev. B **54**, 11169 (1996).
- [33] G. Kresse and J. Furthmüller, Comput. Mater. Sci. **6**, 15 (1996).
- [34] G. Kresse and D. Joubert, Phys. Rev. B **59**, 1758 (1999).
- [35] J.P. Perdew, K. Burke, and M. Ernzerhof, Phys. Rev. Lett. **77**, 3865 (1996).
- [36] J. Heyd, G.E. Scuseria, and M. Ernzerhof, J. Chem. Phys. **125**, 224106 (2006).
- [37] G. Mills and H. Jonsson, Phys. Rev. Lett. **72**, 1124 (1994).
- [38] J. Ma and S.-H. Wei, Phys. Rev. Lett. **110**, 235901 (2013).
- [39] H. Wolf, F. Wagner, Th. Wichert, and Isolde Collaboration, Phys. Rev. Lett. **94**, 125901 (2005).
- [40] E.D. Jones, N.M. Stewart, and J.B. Mullin, J. Cryst. Growth **117**, 244 (1992).

[41] T. Fan and I. Sankin, unpublished.

[42] S.-H. Wei, *Comput. Mater. Sci.* **30**, 337 (2004).

Figures

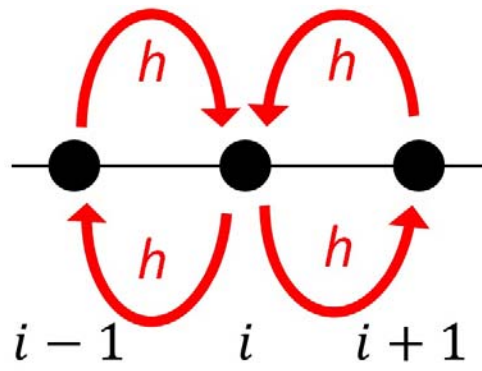


FIG. 1 (color online). One-barrier diffusion with particle hopping rate h between neighboring sites.

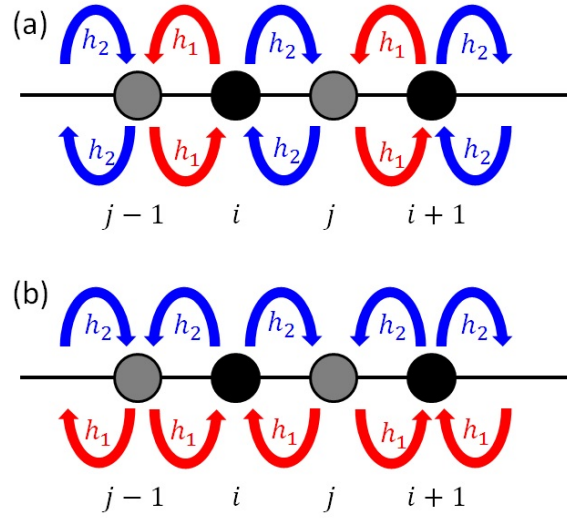


FIG. 2 (color online). Two types of diffusions with two barriers. (a) Hopping between neighboring sites is symmetric, but hopping for one full diffusion path is not symmetric (Type I); (b) Hopping between neighboring sites is not symmetric, but hopping for one full diffusion path is symmetric (Type II). Note that from the periodic view, both types are symmetric because the diffusion medium is uniform.

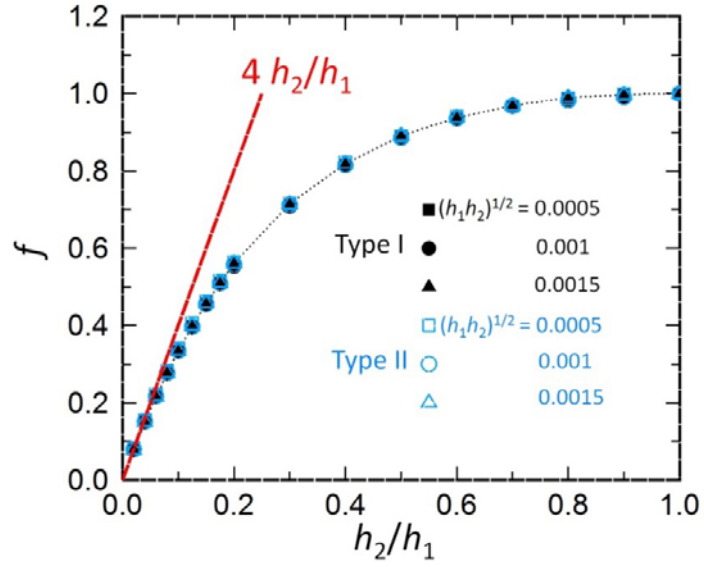


FIG. 3 (color online). MC simulated results of f . At $h_2/h_1 = 1$, $f = 1$ and at $h_2/h_1 < 0.15$, $f = 4h_2/h_1$. Note that f depends only on the ratio of h_2/h_1 ($h_2 < h_1$), but not on the absolute values of h_1 and h_2 . The geometric means of h_1 and h_2 are given in arbitrary unit.

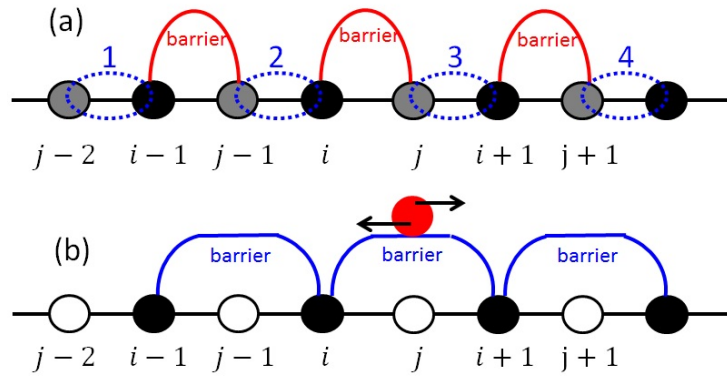


FIG. 4 (color online). (a) Type-I and (b) type-II diffusion pathways in the limit $h_2 \ll h_1$.

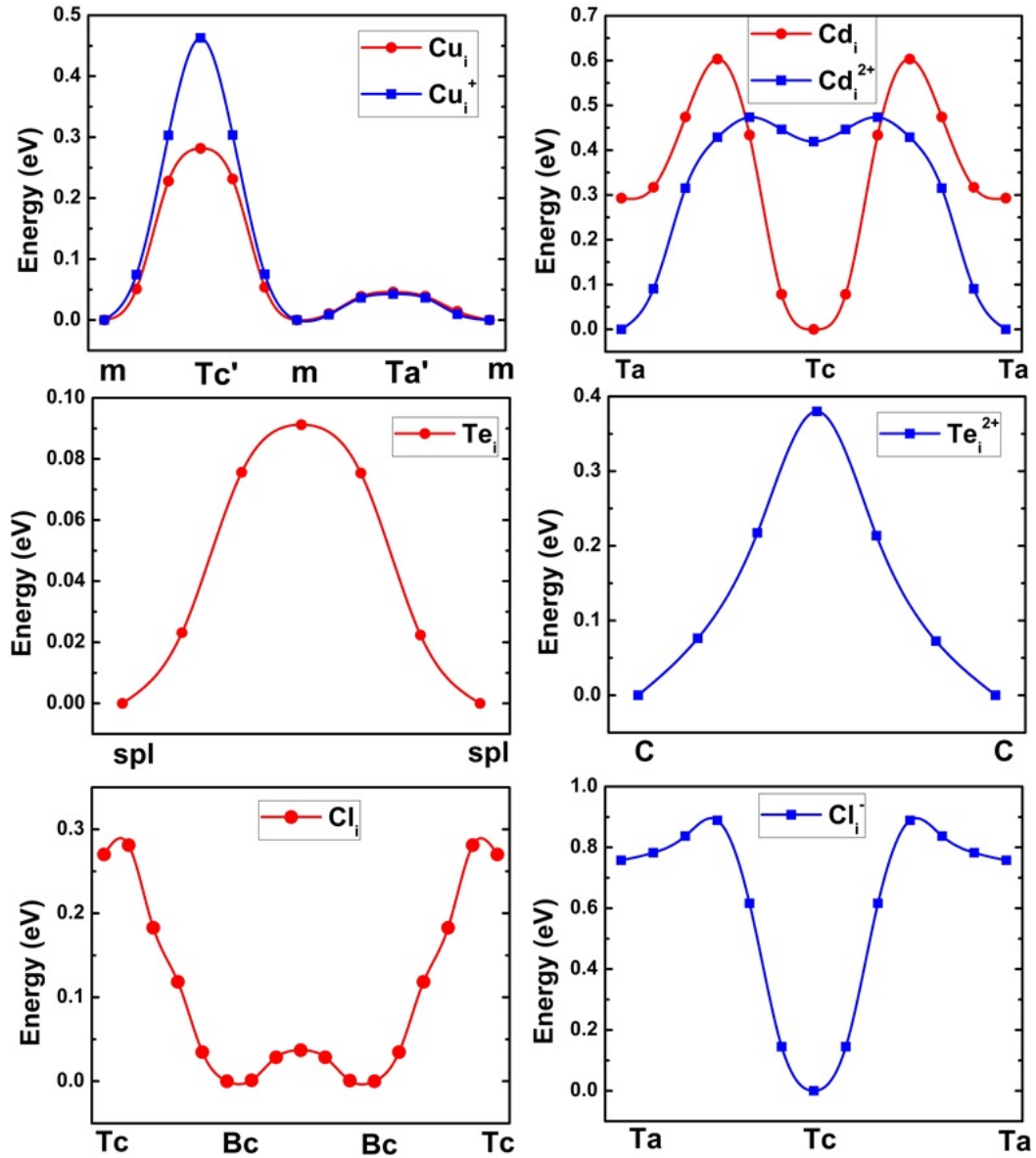


FIG. 5 (color online). Full diffusion paths of Cu_i , Cd_i , Te_i , and Cl_i in their neutral and charged states in CdTe, calculated by the NEB method with bandgap corrected by HSE06 functionals.

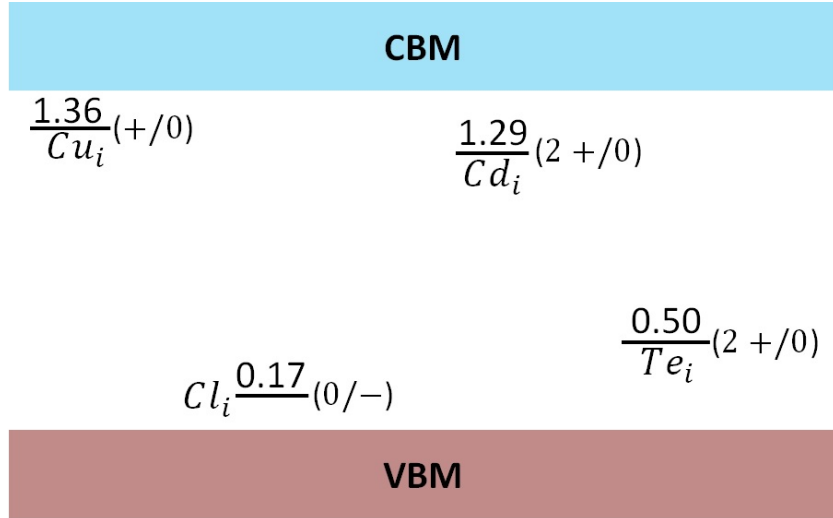


FIG. 6 (color online). Defect transition energy levels of Cu_i , Cd_i , Te_i , and Cl_i , referenced to VBM of CdTe calculated using HSE06 according to Ref. 42. The calculated bandgap is 1.5 eV using the HSE06 functional.

Table 1. Calculated diffusion energy barriers E_a , diffusion lengths a , number of equivalent diffusion sites z , attempting frequencies μ associated with E_a , and effective diffusion coefficient pre-factors D_0 . Here, E_a is the highest barrier among a full diffusion path, which is also the effective barrier at a not too high temperature. The listed diffusion coefficient pre-factors are effective values for the full diffusion paths with effective barriers E_a , as are discussed in the text.

defect	E_a (eV)	a (Å)	z	μ (THz)	D_0 (cm^2/s)
Cu_i	0.28	5.03	4	4.19	3.53×10^{-3}
Cu_i^+	0.46	5.03	4	7.47	6.30×10^{-3}
Cd_i	0.60	5.67	4	4.85	5.20×10^{-3}
Cd_i^{2+}	0.47	5.67	4	3.00	3.21×10^{-3}
Te_i	0.09	4.45	6	0.28	5.54×10^{-4}
Te_i^{2+}	0.38	2.91	6	2.14	1.81×10^{-3}
Cl_i	0.28	5.20	4	1.07	4.82×10^{-4}
Cl_i^-	0.89	5.67	4	10.99	1.18×10^{-2}